CrystEngComm

PAPER

View Article Online
View Journal

Cite this: DOI: 10.1039/c6ce00550k

Theoretical description of the role of amine surfactant on the anisotropic growth of gold nanocrystals†

Hongjun You,*[a] Xiaotong Liu,[a] Hongzhong Liu[b] and Jixiang Fang*[a]

Amine molecules are very commonly used surface agents in the shape-controlled synthesis of nanocrystals. In the case of amine-mediated synthesis of Au nanowires, the roles of the amine molecules were studied using theoretical calculation and correspondingly, the mechanism for the anisotropic growth of Au nanowires is discussed. Two features of amine molecules as surfactants in the synthesis system for colloid nanocrystals were found and deeply studied. One feature is the self-assembly of amine molecules induced by the strong interaction between the long carbon-chains. The theoretical calculation result shows that the interaction energy between amine molecules becomes larger when the carbon chain length increases. This result indicates that the amine molecules with longer carbon chains more preferentially self-assembly through their carbon-chains as they adsorb onto nanoparticles. The other feature is the large difference of adsorption energies on the Au (100) and (111) facets. These two features of the oleylamine molecules play important roles on the anisotropic growth of Au nanocrystal along the <111> direction. This study will help to further understand the functions of amine molecules in the synthesis of colloidal nanocrystals.

Received 10th March 2016,
Accepted 26th April 2016

DOI: 10.1039/c6ce00550k

www.rsc.org/crystengcomm

Introduction

One-dimensional (1-D) metallic nanocrystals have attracted explosive interest because of their unique properties and potential applications in nanoelectronics, photonics, magnetics, sensors and catalysis.[1–9] Blossoming from the studies was enabled by chemical breakthroughs that allowed the reproducible and affordable synthesis of nanowires (NWs) or nanorods.[10–16] To obtain a 1-D nanostructure, the intrinsic isotropic growth behavior of the metallic crystal should be destroyed.[11,12] The general mechanism of anisotropic growth involves template limited growth, ligand controlled growth, defects in seed-induced anisotropic growth, and oriented attachment.[17–25] These growth mechanisms are mainly deduced from experimental observation; however, systematic theoretical studies are still scarce.[11,26,27] Combined with experimental methods, theoretical studies help deeply disclose and understand the growth mechanism.[12] For example, the growth process of gold nanorods in halides, silver, and surfactant systems was discussed based on theoretical calculation results using density functional theory (DFT).[28]

Since ultrathin Au NWs were synthesized in an oleylamine (OAm) assisted system, they have attracted considerable attention because of their high aspect ratio and simple synthesis protocol.[29–37] Several growth mechanisms based on experimental observations have been proposed. The Xia group reports that OAm may assemble the Au(I) ions into 1-D polymeric chains through formation of a [(OAm)AuCl] complex. When the Au(I) is converted to Au(0) under slow reduction conditions, the nucleation and growth of Au can be mediated by the 1-D polymer strands to generate ultrathin NWs.[30] The Yang group's study shows that the micelle formed by the Au(I)–OAm complex serves as a growth template to govern the anisotropic growth.[32] However, these studies still have not completely and deeply disclosed the anisotropic growth mechanism of Au NWs. For example, the question of why the Au NWs growing along the <111> directions through (111) facets has not been well explained. Usually, the (111) facets are the most stable surface for the *fcc* (face-centered cubic) noble metal nanocrystals, so the preferential growth along the <111> directions is inconsistent with this crystal growth behavior. Halder and Ravishankar propose that the OAm surfactant is preferentially removed from the (111) planes, thus resulting in the assembly of truncated-octahedral Au nanoparticles through (111) planes to form NWs.[29] Actually, the

[a] School of Science, State Key Laboratory for Mechanical Behavior of Materials, Xi'an Jiaotong University, Shannxi 710049, PR China.
E-mail: hjyou@mail.xjtu.edu.n, jxfang@mail.xjtu.edu.cn
[b] School of Mechanical Engineering, Xi'an Jiaotong University, Shannxi 710049, PR China

† Electronic supplementary information (ESI) available: TEM image for Au nanocrystals obtained at the beginning of synthesis. Figures for the relation of interaction energy of molecules *vs.* double bond position and DOS of d-band electrons for different facets. Tables for d-band center, adsorption energy of ammonia and methylamine molecules on a Au surface, and surface energies of different metal surfaces. See DOI: 10.1039/c6ce00550k

truncated-octahedral Au nanoparticle has eight (111) surfaces. There are four possible directions for the growth of nanocrystal through oriented attachment of Au nanoparticles. Thus, wormlike NWs, rather than straight NWs, should be obtained by nanoparticle aggregation as described in from other report.[11,38,39] Herein, by combining theoretical calculations and experimental observations, the roles that OAm plays on the formation of Au NWs are descripted, and correspondingly, the anisotropic 1-D growth of Au nanocrystals along one dimension is discussed. OAm is a kind of long-chain primary alkylamine and is a widely used reagent for the synthesis of various metallic, metal-oxide, and semiconductor nanostructures with wet chemistry in organic solvents.[40] Commercial OAm has a much lower cost than other commonly used pure alkylamines, though some concerns regarding purity and reproducibility have also been raised. Moreover, OAm is a liquid at room temperature, and thus, it may act both as surfactant and solvent. This study will not only disclose the anisotropic growth mechanism of Au NWs under OAm direction, but also help to further understand the roles of OAm as a surfactant for the chemical synthesis of metal nanocrystals.

Methods

Synthesis and characterization of Au nanowires

The synthesis of Au NWs was performed by the Yang group's method.[32] In the procedure, 0.058 g $HAuCl_4{\cdot}3H_2O$ and 20 mL OAm were mixed together by ultrasonication for 15 min. The resulting transparent solution was aged at room temperature for 4 days. Finally, purple precipitate was formed and was separated by centrifugation at 5000 rpm for 10 min. The product was washed 4 times with a mixed solution of toluene (2 mL) and ethanol (6 mL). The produced Au nanowire was dispersed in chloroform for further characterization. The transmission electron microscopy (TEM) and high-resolution transmission electron microscopy (HRTEM) analysis images were performed on a JEOL JEM-2100 transmission electron microscope operating at an accelerating voltage of 200 kV.

Calculation and simulation

The configurations of OAm molecule-aggregation was performed in a Forcite package with the PCFF30 force field describing the interaction of the molecules and was similar with our previous report.[41,42] The force field of PCFF30 was based on the *ab initio* principle and empirical parameters.[43,44] The configurations of different numbers of OAm molecules were optimized with static calculations (*i.e.*, geometry optimization at 0 K). The geometry optimizations were defined to be converged under the following criteria: the energy tolerance being less than 2.0×10^{-5} kcal mol^{-1} and the maximum displacement being less than 1.0×10^{-5} Å using a smart algorithm.

The stability of the Au NWs was studied using molecular dynamics (MD) simulations. The MD simulations were also performed in the Forcite package with the PCFF30 force field. The simulation temperature and simulation time were 300 K and 200 ps, respectively.

The adsorption energies of amine molecules on Au, Ag, Pt, and Pd crystal surfaces and the surface energies of Au, Ag, Pt, and Pd metals were calculated using a similar DFT method to our previous report.[45] The DFT calculation was performed with the Dmol3 code that was developed by Delley.[46] The adsorption structures were optimized using the Perdew–Wang exchange-correlation function (PW91) based on the generalized gradient approximation. No symmetry and spin restrictions were applied. A double numerical basis set with a polarization p-function, DFT semicore pseudopots, and an octupole scheme was selected to describe the multipolar expansion of the charge density and the Coulomb potential. The following criteria were used to obtain the optimized final structure. First, the convergence tolerance of the self-consistent field energy was less than 10^{-6} hartree (Ha) in the conjugate gradient algorithm. Second, the maximum displacement of an atom was less than 0.005 Å, and the force due to the displacement was less than 0.002 Ha $Å^{-1}$. The structures of both the ligand molecules and the crystal surfaces were fully optimized before they were brought together. Subsequently, the entire structure containing the adsorbed ligand molecules and crystal surfaces was optimized to obtain the most stable form. The adsorption energy (E_a) was then obtained using the following equation:

$$E_a = E_{total} - E_s - E_m$$

where E_{total}, E_s, and E_m are the bond energies of the whole system, crystal surface, and free molecules, respectively.

Results and discussion

The OAm assisted synthesis of ultrathin Au NWs is very simple in which only two additives are included, *i.e.* OAm and $HAuCl_4$. Using a similar method to the Yang group's report,[32] we synthesized the Au NWs. The TEM image in Fig. 1a shows that the Au NWs are uniform and ultrathin in diameter (about 1.8 nm), and have very high length and diameter ratios. The lattice space obtained from the HRTEM image in Fig. 1b is 0.23 nm, which matches with Au {111} planes *d*-spacing. Same to the previous report, the Au NWs are single crystalline entities and grow along the <111> direction.[32] Using the same method as Strasser group's report,[47] it can be deduced from the relationship of low index facets in *fcc* crystal (Fig. 1c) that the Au NWs are bounded by (100) facets (Fig. 1b). This result is consistent with Halder and Ravishankar's report.[29] The crystal structure of Au NWs is shown as the model image in Fig. 1d and e. The growth process of Au NWs was also investigated by analysing the sample taken from the reaction mixture at the beginning stage using TEM characterization. Same as with Halder and Ravishankar's report,[29] at the first stage of the Au NWs growth process, nanoparticles with a size of 1 to 2 nm were mainly obtained (Fig. S1†).

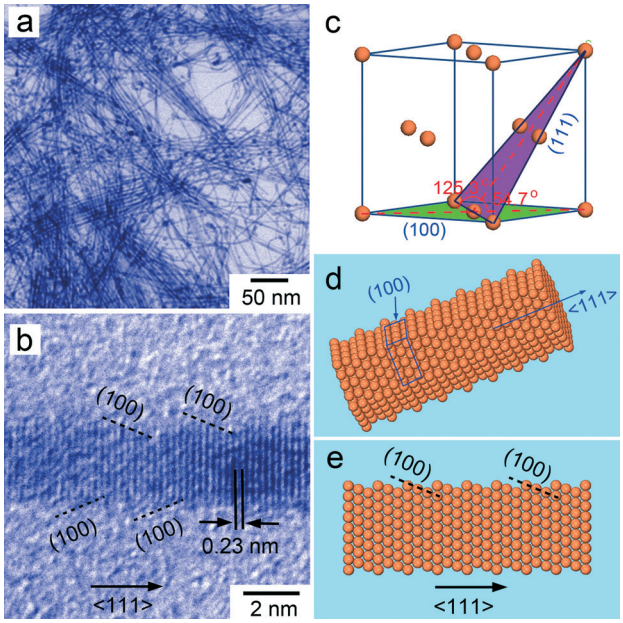

Fig. 1 TEM and structure images of Au NWs: (a) TEM, (b) HRTEM, (c) crystal structure, (d) 3D model, and (e) 2D model images of Au NWs.

The synthesis of ultrathin Au NWs contains three ingredients, *i.e.* OAm molecule, Au^{3+} ions and Cl^- ions. The Cl^- ion are endothermically adsorbed onto the Au surface:[28] therefore, over-layers of Cl^- ions would be too labile to block surface growth due to rapid adsorption/desorption processes.[28] The Au^{3+} ions provide Au atoms for NW growth through reduction by OAm molecules. The OAm molecules perform both the role of reducing agent and of surfactant that shows a crucial role on the formation of Au NWs. It was reported that in other synthesis systems containing OAm, Au NWs can also be obtained.[33–36] Following of the function of OAm molecules as surfactants in the Au NWs formation process were systematically studied using MD simulations and DFT calculations. Based on the result, the roles that the OAm molecule performs on the anisotropic growth of Au NWs are discussed.

Firstly, the interactions between OAm molecules were calculated using a similar method to the previous report.[41,42] Fig. 2 shows the final optimized configurations of OAm molecules. When 2 to 7 OAm molecules were put together, they will self-assemble with each other. In their optimized configurations, the carbon chains are parallel, close together, and attractions are formed between each chain. When two OAm molecules were put together, the interaction energy gain (absolute value of interaction energy) formed between them was 0.24 eV. When the number of OAm molecules increased to more than 2, the average interaction energy gain between any two molecules increases to 0.48 eV and keeps stable in the systems with 3, 4, and 7 molecules. As a surfactant in actual synthesis, the adsorbed molecules on a nanocrystal could be more than 2, thus, the interaction energy gained from between any two OAm ligand molecules should be around 0.48 eV. The function of the carbon chain of OAm was further studied by changing the length of the carbon chain. As shown in Fig. 3, with the carbon-chain length decreasing from 18 (OAm) to 0 (ammonia), the interaction energy gain between molecules decreases from 0.48 eV to nearly 0.10 eV. When the carbon-chain length is less than 4 carbon atoms, the interaction energy of −0.10 eV mainly comes from the hydrogen bond formed between two amine groups. The interaction between carbon chains should be almost 0. For the carbon-chains with more than 4 carbon atoms, the interaction quickly rises with increasing carbon chain length. When the carbon chain increases to more than 14 carbon atoms, the increase of interaction energy slows. This result indicates that the amine molecules with longer carbon-chains are more preferentially self-assembled through their carbon-chains as they adsorb on the surface of nanocrystals.

In order to keep consistent with the structure of OAm molecules, in the geometry optimization for the assembly of

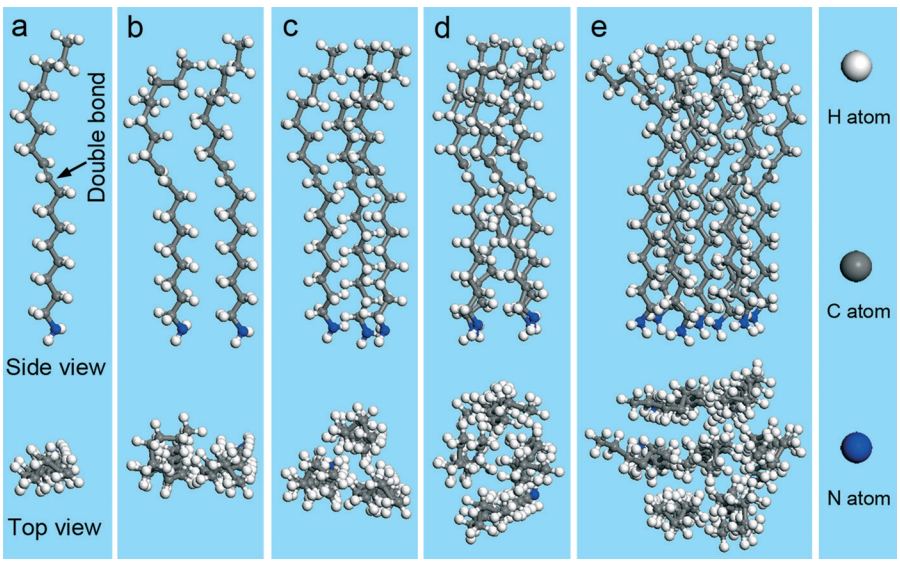

Fig. 2 Optimized configurations of OAm molecules: (a) single OAm molecule, (b) 2, (c) 3, (d) 4 and (e) 7 OAm self-assembled molecules.

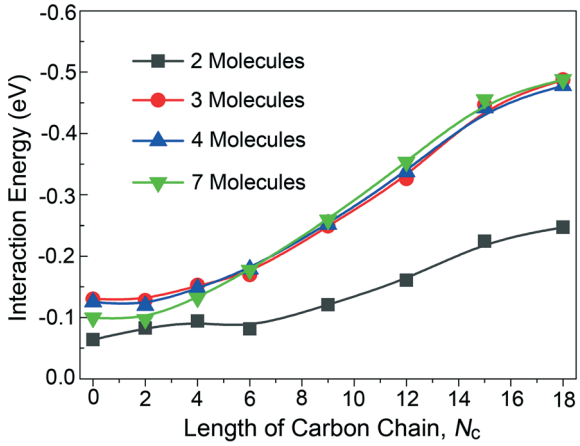

Fig. 3 Interaction energy of each amine molecule when it self-assembles into 2, 3, 4 and 7 molecule groupings with the length of carbon-chain increasing from 0 to 18 carbon atoms.

amine molecules with different carbon chain lengths, one double bond is contained and located at the middle of the carbon chain. The effect of the position of the double bond on the interaction energy between amine molecules was studied. As shown in Fig. S2,† when the position of the double bond changes from the 1st to 17th carbon, the interaction energy between molecules fluctuates between −0.43 to −0.53 eV. This result indicates that the position of the double bond in the carbon chain has no obvious effect on the interaction between amine molecules.

Secondly, the adsorptions of OAm molecules on different facets of the noble metal nanocrystal were calculated using DFT. Similar with previous reports,[38] the calculation was simplified by using a shorter carbon chain molecules, propylamine, to model the functional group of OAm. Au (100), (111), and (110) surfaces are set in a 2 × 2 periodic cell. Fig. 4 shows the side and top views of the most likely configurations of amine molecules on the Au (111), (100) and (110) facets, which were fully optimized based on DFT. The DFT

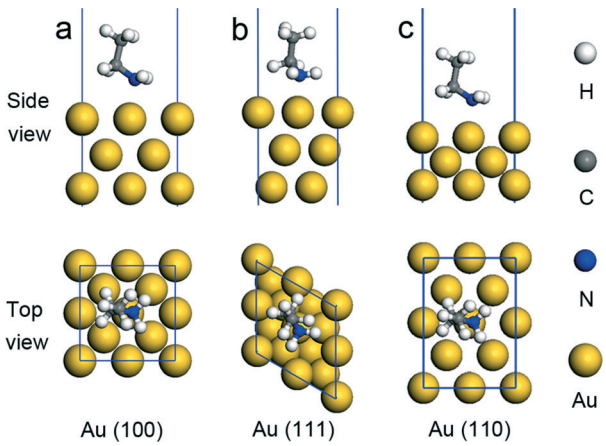

Fig. 4 Optimized configurations of an amine molecules adsorbed on (a) Au (100), (b) Au (111), and (c) Au (110) surface in a periodic cell using DFT method.

optimized configurations of amine groups on other noble metals (Ag, Pd, and Pt) surfaces were very similar with that of the Au surface. The amine group adsorbs exclusively with a single metal atom at a top site *via* its nitrogen atom; no binding is found on all of the high-symmetry sites. The N atom locates at the top of the C–N–H_2 tetrahedron and connects with a solo Au atom. The adsorption energies of amine group adsorbed on (111), (100), and (110) facets of Au, Ag, Pd, and Pt metals are shown in Table 1. An interesting result can be found from the data in Table 1. Unlike Ag, Pd, and Pt, the adsorption energy gain (absolute value of adsorption energy) of amine group on the Au (100) facet is much higher than that on the Au (111) facet and their ratio ($E_a^{(100)}/E_a^{(111)}$) reaches 2.08. However, the ratios of $E_a^{(100)}/E_a^{(111)}$ for metals of Ag, Pd, and Pt are 1.46, 1.06 and 1.18, respectively (Fig. S3†). This result indicates that for the Au metal, the amine molecules will preferentially adsorb onto the Au (100) facets than onto the (111) facets. Compared with Au metal, the difference of adsorption energy for amine molecules on Ag (100) and (111) surfaces is little, and that for Pd and Pt metals are not obvious.

Fig. 5 shows the electron density distribution when the amine molecules adsorb onto the Au (100), (111), and (110) facets. The intensity of interaction between the amine group and the Au surface can be rationalized by the electron density distribution in the electron clouds formed between the amine group and the Au atom. The Au atom connects with the N atom along the top direction of the C–N–H_2 tetrahedron to form the maximum electron cloud overlap. The isosurface of the electron density distribution with a value of 0.2 electrons per $Å^3$ shows that the neck between N and Au atoms is narrower for the amine molecules adsorbed on the Au (111) surface than that for amine adsorbed on the Au (100) and (110) surfaces (Fig. 5a–c). From the center-slice maps of the electron density distribution (Fig. 5d–e), it can be found that the degree of electron cloud overlap between Au and N atoms for the amine molecules adsorbed on Au (111) is lower than that on the Au (100) and (110) surfaces. From the slice map crossing the electron cloud neck between Au and N atoms (Fig. 5g–i), it also can be found that the density of electrons for the amine molecules adsorbed on Au (111) is lower than that on the Au (100) and (110) surfaces. This result indicates that the amine group forms a stronger interaction with the Au (100) and (110) surfaces than the (111) surface.

The chemical adsorption of molecules onto a noble metal surface is related to the valence electrons of the metals. The

Table 1 Adsorption energies (E_a) of an amine molecule, obtained from DFT calculations, onto noble metal (100), (111) and (110) surfaces (unit: eV)

Noble metal	$E_a^{(100)}$	$E_a^{(111)}$	$E_a^{(110)}$	Ratio of $E_a^{(100)}/E_a^{(111)}$
Au	−0.608	−0.292	−0.622	2.08
Ag	−0.499	−0.341	−0.501	1.46
Pd	−0.766	−0.724	−0.852	1.06
Pt	−1.05	−0.892	−1.21	1.18

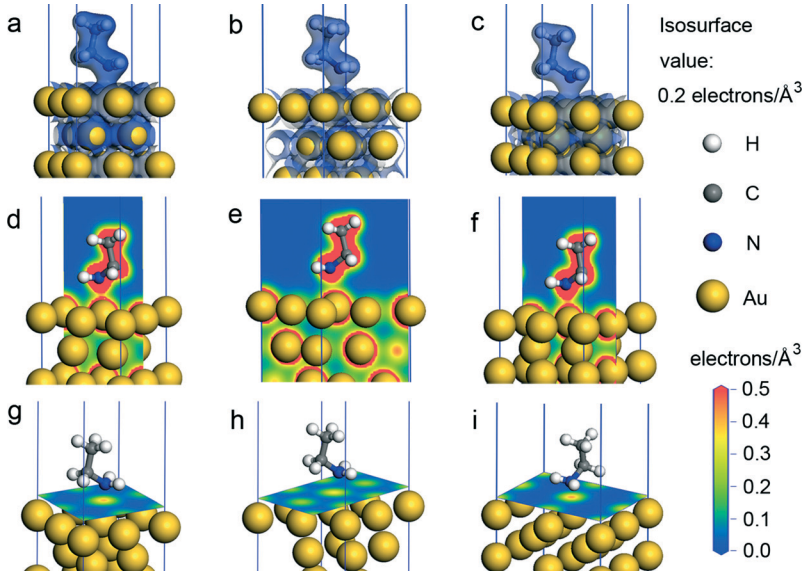

Fig. 5 Distributions of electron density when an amine molecule is adsorbed on (a, d, g) Au (100), (b, e, h) Au (111), and (c, f, i) Au (110) crystal surfaces. (a–c) The isosurfaces of electron density with a value of 0.3 electrons per Å^3. (d–f) The center slices of electron density distributions. (g–i) The slice map crossing the electron cloud neck between Au and N atoms.

density of state (DOS) of d-band electrons for noble metals (Au, Ag, Pd, and Pt) (100) and (111) surfaces was calculated using DFT and the result is shown in Fig. S4.† The values of the d-band center positions obtained from the DOS analysis are shown in Table S1.† It can be found that the difference of d-band centers for the Au (100) and (111) surfaces is higher than the DOS for Ag, Pd, and Pt metals. This result is coincident with the phenomenon in Table 1 that Au metal possesses a higher ratio of $E_a^{(100)}/E_a^{(111)}$ than Ag, Pd, and Pt metals.

The adsorption of ammonia and methylamine molecules on Au (100), (111), and (110) surfaces were also calculated using the same method as the adsorption of propylamine. The results are shown in Table S2.† Compared with propylamine, although the adsorptions of ammonia on Au surfaces are weaker, the their sequence ($E_a^{(110)} > E_a^{(100)} > E_a^{(111)}$) is the same and the ratio of $E_a^{(100)}/E_a^{(111)}$ are close (2.16 for ammonia and 2.08 for propylamine). For methylamine, the difference of adsorption energy compared with propylamine is insignificant. For example, the $E_a^{(110)}$ for methylamine and propylamine are −0.628 eV and −0.622 eV, respectively, for a difference less than 1%. This result indicates that the adsorption properties of surfactant molecules are mainly determined by the functional groups.[45]

Thirdly, the stability of Au NWs was studied using MD simulations. Fig. 6 shows the snapshot of Au NWs with different diameters before and after being relaxed at a temperature of 300 K for 200 ps by MD simulation. For the NWs with diameters of 0.8 nm and 1.2 nm, after 200 ps simulation, they transformed into nearly spherical nanoparticles. When the diameter of NWs increased to more than 1.6 nm, the NWs became stable. After 200 ps simulation, the morphology of the NWs still had no obvious change. So, the diameter of 1.6 nm may be the theoretically threshold value for stable Au NWs. This result is consistent with experimental reports. For example, the diameters of Au NWs synthesized by the Xia, Yang, and Xing groups are 1.8 nm, 1.6 nm, and 1.8 nm, respectively.[30,32,35]

Based on experimental observations and theoretical calculations, the following growth process for Au NWs in the OAm-mediated synthesis system can be proposed. As shown in Fig. 7, the growth may include four steps. Identical to the Yang and Xia groups' reports,[30,32] in the first step, an ordered mesostructure is formed by the complex of Au^+/Au^{3+} ion-OAm

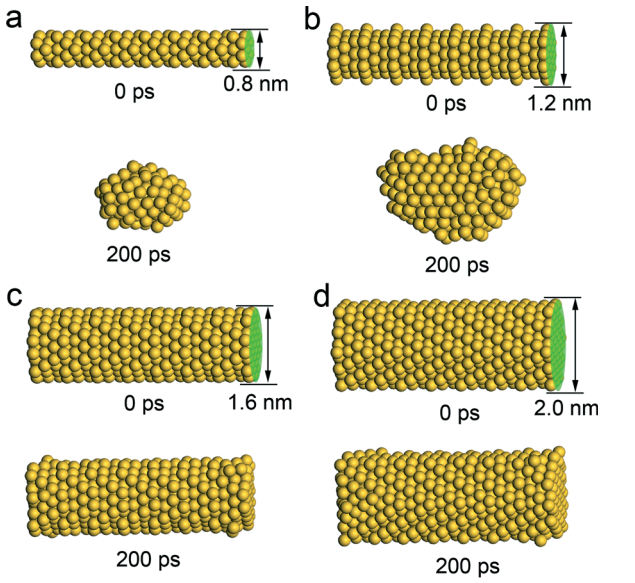

Fig. 6 MD simulation result of Au nanowires after 200 ps with different diameters: (a) 0.8 nm, (b) 1.2 nm, (c) 1.6 nm, and (d) 2.0 nm.

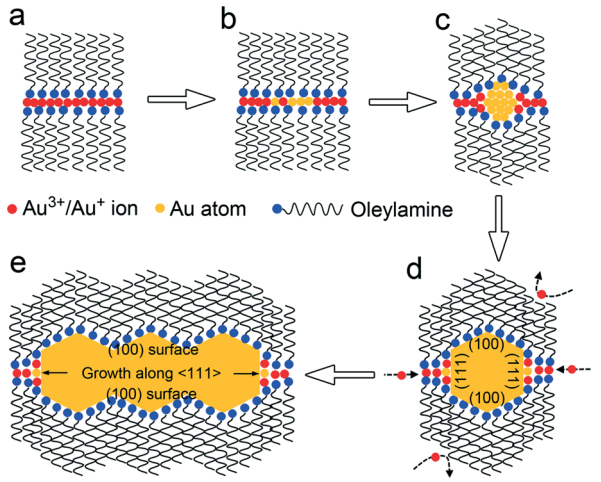

Fig. 7 Schematic of Au NW growth. (a) Micelle structure is formed between Au ions and OAm molecules. (b) Some Au ions are reduced into Au atoms. (c) Au atoms aggregate to form a nucleus. (d) Au nucleus grows into a nanocrystal bounded by (100) and (111) surfaces. (e) Au nanocrystal grow along the <111> direction to form NW.

due to the self-assembling of OAm molecules. As indicated in the previous calculation (Fig. 2 and 3), the carbon chains of OAm molecules may self-assemble due to the strong interactions formed between the long carbon-chains of OAm. The polar amine groups adsorb with Au^{+}/Au^{3+} ions. Thus, a micellar mesostructure, as shown in Fig. 7a, is formed. This mesostructure has been confirmed by the small-angle X-ray diffraction and the small angle X-ray scattering spectra in experiments by the Yang research group.[32]

In the second step, the Au^{+} ions in the micelle are gradually reduced into Au atoms (Fig. 7b). Dependant on the MD simulation result in Fig. 6, the produced Au atoms could not form a stable Au line with ultra-thin diameters less than 1.6 nm. Thus, the produced Au atoms diffuse in the micelle and aggregate together to form a nucleus (Fig. 7c).

In the third step, the Au nuclei grow with the addition of diffused Au atoms to form stable nanoparticles with sizes 1–2 nm as we observed during the first stage of experimental synthesis (Fig. S1†). As in Halder and coworker's report,[29] the produced Au nanoparticles at the beginning of the formation of Au NWs show a truncated octahedral shape and are bounded by low-index (100) and (111) facets. Our DFT calculation indicates that the (111) facets have the lowest surface energies (Table S3†) and the OAm molecules are more preferentially adsorbed onto the Au (100) surface than on the Au (111) surface (Table 1). This result may explain the experimental observation that the beginning nanocrystals are bounded by both (100) and (111) surfaces. Compared with the (110) surface, the surface energy ratio between the (110) and (100) surfaces ($E_s^{(110)}/E_s^{(100)}$) is 1.07, while the adsorption energy ratio of amine molecules on them is only 1.02 less than 1.07. This result shows that in the amine molecules mediated system, the (100) surface is more stable than the (110) surface and the obtained nanocrystals are more preferentially bounded by the (100) facet than the (110) facet.

In the last step, the truncated octahedral Au nanoparticles will transform to NWs through an anisotropic growth. The key question to be explained is how the isotropic growth behavior of the *fcc* Au nanocrystal is destroyed and how the anisotropic growth along the <111> direction is formed. Our calculation result (Fig. 2) shows that the carbon chains of OAm molecules will self-assemble together and as surfactant, they will form a compact wall to prevent the diffusion of Au atoms and ions through them to attach the surface of Au nanocrystals. This role of surfactant can promote the anisotropic growth of metal nanocrystals, similar to cetyltrimethylammonium bromide (CTAB) and dihydroxyphenylalanine (DOPA) molecules.[28,42] As a surfactant, the top of the CTAB molecule (*i.e.* ammonium bromide group) adsorbs onto the Au nanocrystal surface and the tails of the molecules (*i.e.* long carbon chain) will aggregate together.[28] For the DOPA surfactant, due to the hydrogen bonds, the tails of the molecules will also aggregate together.[42] The aggregation of the surfactant tails prevents the metal ions or atoms from diffusing through them to deposit onto the nanocrystal surface they are bound to. Thus, the anisotropic growth along the certain directions will be promoted by the direction of the surfactant molecules.[41,48] On the other hand, our DFT calculation indicates that the OAm are more preferentially adsorbed on the Au (100) surface than on the Au (111) surface (Table 1). As shown in Fig. 7d, a micellar structure may be formed under both functions of selective adsorption and self-assembly of OAm. Due to fact that the Au (111) facet is weakly wrapped by OAm molecules, Au atoms and ions can diffuse along the micelle channel to the (111) surface. With the Au ions/atoms diffusion to the (111) surface, the Au nanocrystals will grow along the <111> direction to form ultra-long NWs (Fig. 7e).

For the other noble metals such as Pd and Pt, the (100) and (111) facets have the lowest surface energy (Table S3†), but the adsorption energies of OAm on the (100) and (111) facets are close (ratios of $E_a^{(100)}/E_a^{(111)}$ are 1.06 and 1.18, respectively). Thus, anisotropic growth hardly occurs, as shown in Fig. S5a,† and only nanoparticles will be obtained. For the Ag metal, the ratio of $E_a^{(100)}/E_a^{(111)}$ is 1.46, lower than Au and higher than Pd and Pt. It is possible for Ag to form NWs, but harder than Au. Currently, in the only amine surfactant-mediated synthesis, linear Pd and Pt NWs have not been reported, and AgAu bimetallic NWs have been synthesized using octadecylamine as a surfactant.[49] On the other hand, for the amine molecules with short carbon-chains, the weak interaction between carbon-chains cannot induce the self-assembly of molecules to form micelles that promote the anisotropic growth of nanocrystals along certain orientations. Thus, as illustrated in Fig. S5b,† NWs are hardly formed using amine molecules with short carbon-chains as a surfactant.

Conclusions

In summary, from the theoretical calculation, we find two important features of amine molecules as surfactant in the

synthesis of metal nanocrystals. One feature is the self-assembly of amine molecules with long carbon-chains. They will act as a compact wall through strong interactions formed between the carbon-chains to prevent the diffusion of metal atoms and ions through them. Thus, they direct the growth of metal nanocrystals along certain directions. The other feature is the selected adsorption on different metal crystal facets. The preferential adsorption of OAm on the (100) surface will promote the anisotropic growth of Au NWs along the <111> orientation. This study, for these two features, may help further deeply understand the roles of amine molecules as surfactants in metal nanocrystal synthesis.

Acknowledgements

This work was supported by National Natural Science Foundation of China (no. 51201122 and 51171139), Doctoral program of higher education of China (no. 20120201120049), and Fundamental Research Funds for the Central Universities.

Notes and references

1 S. J. Guo, S. Zhang, X. L. Sun and S. H. Sun, *J. Am. Chem. Soc.*, 2011, **133**, 15354.
2 C. Koenigsmann, W. P. Zhou, R. R. Adzic, E. Sutter and S. S. Wong, *Nano Lett.*, 2010, **10**, 2806.
3 B. Y. Xia, H. B. Wu, Y. Yan, X. W. D. Lou and X. Wang, *J. Am. Chem. Soc.*, 2013, **135**, 9480.
4 M. Grzelczak, J. Perez-Juste, P. Mulvaney and L. M. Liz-Marzan, *Chem. Soc. Rev.*, 2008, **37**, 1783.
5 A. Kisner, M. Heggen, D. Mayer, U. Simon, A. Offenhausser and Y. Mourzina, *Nanoscale*, 2014, **6**, 5146.
6 A. Bezryadin, C. N. Lau and M. Tinkham, *Nature*, 2000, **404**, 971.
7 X. Huang, S. Neretina and M. A. El-Sayed, *Adv. Mater.*, 2009, **21**, 4880.
8 U. Yogeswaran and S. M. Chen, *Sensors*, 2008, **8**, 290.
9 Y. Chen, Z. Ouyang, M. Gu and W. L. Cheng, *Adv. Mater.*, 2013, **25**, 80.
10 L. Cademartiri and G. A. Ozin, Ultrathin Nanowires - A Materials Chemistry Perspective, *Adv. Mater.*, 2009, **21**, 1013–1020.
11 H. J. You, S. C. Yang, B. J. Ding and H. Yang, *Chem. Soc. Rev.*, 2013, **42**, 2880.
12 Y. Xia, Y. J. Xiong, B. Lim and S. E. Skrabalak, *Angew. Chem., Int. Ed.*, 2009, **48**, 60.
13 Q. Q. Wang, J. B. Han, D. L. Guo, S. Xiao, Y. B. Han, H. M. Gong and X. W. Zou, *Nano Lett.*, 2007, **7**, 723.
14 E. C. Garnett, W. S. Cai, J. J. Cha, F. Mahmood, S. T. Connor, M. G. Christoforo, Y. Cui, M. D. McGehee and M. L. Brongersma, *Nat. Mater.*, 2012, **11**, 241.
15 A. Morag, V. Ezersky, N. Froumin, D. Mogiliansky and R. Jelinek, *Chem. Commun.*, 2013, **49**, 8552.
16 X. W. Teng, W. Q. Han, W. Ku and M. Hucker, *Angew. Chem., Int. Ed.*, 2008, **47**, 2055.
17 C. Zhu, H.-C. Peng, J. Zeng, J. Liu, Z. Gu and Y. Xia, *J. Am. Chem. Soc.*, 2012, **134**, 20234.
18 H. J. You, F. L. Zhang, Z. Liu and J. X. Fang, *ACS Catal.*, 2014, **4**, 2829.
19 L. H. Shi, A. Q. Wang, Y. Q. Huang, X. W. Chen, J. J. Delgado and T. Zhang, *Eur. J. Inorg. Chem.*, 2012, 2700–2706.
20 X. Hong, D. S. Wang, R. Yu, H. Yan, Y. Sun, L. He, Z. Q. Niu, Q. Peng and Y. D. Li, *Chem. Commun.*, 2011, **47**, 5160.
21 R. Liu, J. F. Liu and G. B. Jiang, *Chem. Commun.*, 2010, **46**, 7010.
22 X. F. Yu, D. S. Wang, Q. Peng and Y. D. Li, *Chem. – Eur. J.*, 2013, **19**, 233.
23 J. T. He, Y. W. Wang, Y. H. Feng, X. Y. Qi, Z. Zeng, Q. Liu, W. S. Teo, C. L. Gan, H. Zhang and H. Y. Chen, *ACS Nano*, 2013, **7**, 2733.
24 C. Morita, H. Tanuma, C. Kawai, Y. Ito, Y. Imura and T. Kawai, *Langmuir*, 2013, **29**, 1669.
25 L. Cheng, C. S. Ma, G. Yang, H. J. You and J. X. Fang, *J. Mater. Chem. A*, 2014, **2**, 4534.
26 T. Yao, S. J. Liu, Z. H. Sun, Y. Y. Li, S. He, H. Cheng, Y. Xie, Q. H. Liu, Y. Jiang, Z. Y. Wu, Z. Y. Pan, W. S. Yan and S. Q. Wei, *J. Am. Chem. Soc.*, 2012, **134**, 9410.
27 C. Zhu, H. C. Peng, J. Zeng, J. Y. Liu, Z. Z. Gu and Y. N. Xia, *J. Am. Chem. Soc.*, 2012, **134**, 20234.
28 N. Almora-Barrios, G. Novell-Leruth, P. Whiting, L. M. Liz-Marzan and N. Lopez, *Nano Lett.*, 2014, **14**, 871.
29 A. Halder and N. Ravishankar, *Adv. Mater.*, 2007, **19**, 1854.
30 X. M. Lu, M. S. Yavuz, H. Y. Tuan, B. A. Korgel and Y. N. Xia, *J. Am. Chem. Soc.*, 2008, **130**, 8900.
31 C. Wang, Y. J. Hu, C. M. Lieber and S. H. Sun, *J. Am. Chem. Soc.*, 2008, **130**, 8902.
32 Z. Y. Huo, C. K. Tsung, W. Y. Huang, X. F. Zhang and P. D. Yang, *Nano Lett.*, 2008, **8**, 2041.
33 N. S. Pazos-Pérez, D. Baranov, S. Irsen, M. Hilgendorff, L. M. Liz-Marzán and M. Giersig, *Langmuir*, 2008, **24**, 9855.
34 Z. Q. Li, J. Tao, X. M. Lu, Y. M. Zhu and Y. N. Xia, *Nano Lett.*, 2008, **8**, 3052.
35 H. J. Feng, Y. M. Yang, Y. M. You, G. P. Li, J. Guo, T. Yu, Z. X. Shen, T. Wu and B. G. Xing, *Chem. Commun.*, 2009, 1984.
36 Y. J. Kang, X. C. Ye and C. B. Murray, *Angew. Chem., Int. Ed.*, 2010, **49**, 6156.
37 C. Wang, Y. Wei, H. Jiang and S. Sun, *Nano Lett.*, 2010, **10**, 2121.
38 Z. M. Peng, H. J. You and H. Yang, *ACS Nano*, 2010, **4**, 1501.
39 S. Hu and X. Wang, *Chem. Soc. Rev.*, 2013, **42**, 5577.
40 S. Mourdikoudis and L. M. Liz-Marzán, *Chem. Mater.*, 2013, **25**, 1465.
41 Z. Liu, F. L. Zhang, Z. B. Yang, H. J. You, C. F. Tian, Z. Y. Li and J. X. Fang, *J. Mater. Chem. C*, 2013, **1**, 5567.
42 Z. B. Yang, L. Zhang, H. J. You, Z. Y. Li and J. X. Fang, *Part. Part. Syst. Charact.*, 2014, **31**, 390.
43 H. Sun, S. J. Mumby, J. R. Maple and A. T. Hagler, *J. Am. Chem. Soc.*, 1994, **116**, 2978.
44 H. Sun, *Macromolecules*, 1995, **28**, 701.
45 H. J. You, W. J. Wang and S. C. Yang, A Universal Rule for Organic Ligand Exchange, *ACS Appl. Mater. Interfaces*, 2014, **6**, 19035–19040.

46 B. Delley, From Molecules to Solids with the DMol(3) Approach, *J. Chem. Phys.*, 2000, **113**, 7756–7764.
47 L. Gan, C. H. Cui, M. Heggen, F. Dionigi, S. Rudi and P. Strasser, *Science*, 2014, **346**, 1502.
48 H. J. You, Y. T. Ji, L. Wang, S. C. Yang, Z. M. Yang, J. X. Fang, X. P. Song and B. J. Ding, *J. Mater. Chem.*, 2012, **22**, 1998.
49 X. Hong, D. S. Wang, R. Yu, H. Yan, Y. Sun, L. He, Z. Q. Niu, Q. Peng and Y. D. Li, *Chem. Commun.*, 2011, **47**, 5160.

